Cover Page

Universiteit Leiden

The handle http://hdl.handle.net/1887/57991 holds various files of this Leiden University dissertation

Author: Rossius, S.G.H.
Title: Q-wires': Synthesis, electrochemical properties and their application in electro-enzymology
Issue Date: 2017-09-26

CHAPTER 5

Electrochemistry of electrode surface-tethered respiratory enzymes

SGH Rossius, MTM Koper, HA Heering

5.1 Introduction

The respiratory chain of *E. coli* is very versatile; it can potentially utilize ten different electron donors and six different electron acceptors [1]. There are many redox enzymes involved in establishing the many possible respiratory pathways. In the presence of a high concentration of oxygen, the cytochrome bo_3 ubiquinol oxidase functions as the predominant terminal oxidase [2]. However, in the absence of oxygen and in the presence of an alternative terminal electron acceptor, *E. coli* can perform anaerobic respiration. Examples of these acceptors are: nitrate; DMSO; TMAO and fumarate [3]. The 'quinone pool' present in the cytoplasmic membrane plays a central role in transporting electrons between the different respiratory complexes [4, 5]. In this study, *E. coli* fumarate reductase, DMSO reductase and cytochrome bo_3 will be studied, which oxidize quinols and function as terminal respiratory complexes. In addition, *E. coli* succinate dehydrogenase will be studied, which participates in the tricarboxylic acid cycle and reduces ubiquinone [6]. For a schematic representation of these enzymes, see figure 2.

In this chapter, the electro-enzymology of the aforementioned four respiratory enzymes will be explored by means of cyclic voltammetry. The 'Q-wires' introduced and characterized in the previous chapters will be employed to provide non-rate-limiting electron transfer between electrode and enzyme. Electrodes decorated with these wires will therefore function as an artificial quinone pool [7] for the enzymes. In addition, alkanethiols will prevent direct contact with the electrode, preventing damage to the enzymes. Figure 1 depicts a

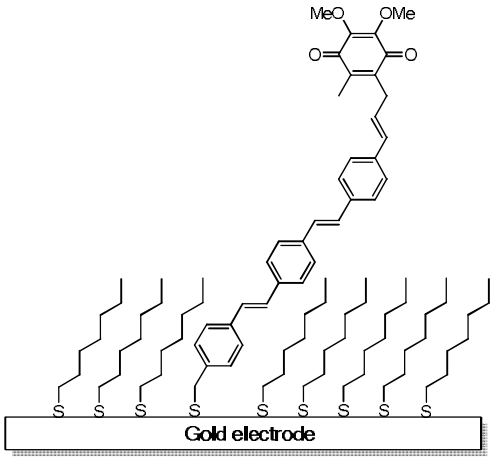

Figure 1 Visualization of the surface of a gold electrode modified with a Q-wire (**U_3**) and heptanethiol

visualization of the electrode surface modifications used for most experiments.

As will be elaborated on below, enzyme activity was indeed observed using the system presented in figure 1, albeit only qualitatively. Poorly reproducible results hindered proper quantitative analysis. Whether the system depicted in figure 1 is therefore useful in meaningful enzymology remains therefore to be decided. Further optimizations are necessary to achieve the full objective of this project.

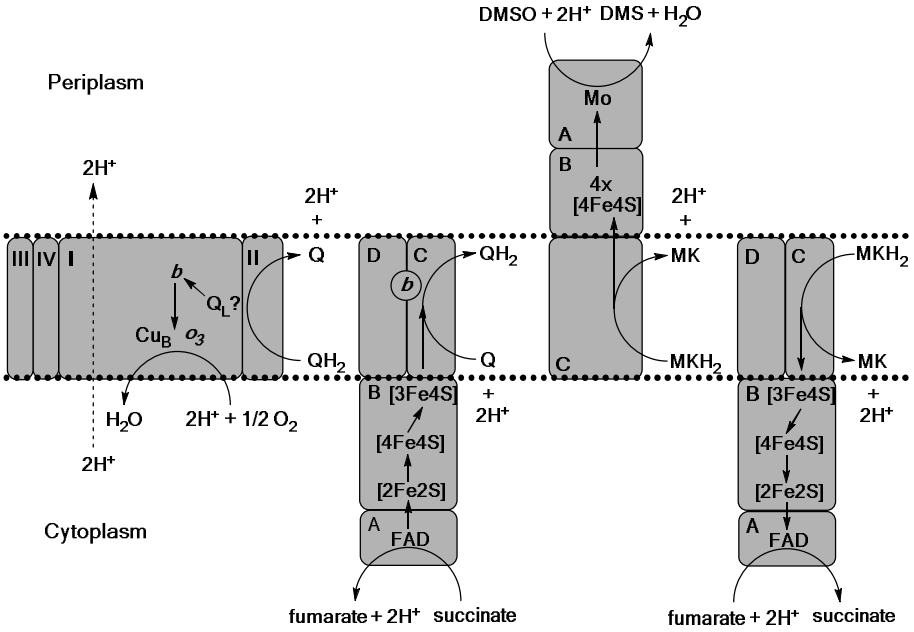

Figure 2 Schematic representation of the membrane-associated *E. coli* redox enzymes addressed in this study, showing their cofactors. Note that co-expression of these enzymes is highly unlikely. From left to right: cytochrome bo_3 (subunit I-IV); succinate dehydrogenase (subunit A-D); DMSO reductase (subunit A-C); fumarate reductase (subunit A-D). The dotted, vertical arrow represents proton pumping; the curved arrows represent electron transfer. Q/QH_2: ubiquinone/ubiquinol; MK/MKH_2: menaquinone/menaquinol. For clarification of the cofactor abbreviations, see text

5.1.1 *E. coli* fumarate reductase and *E. coli* succinate dehydrogenase

Anaerobically expressed *E. coli* fumarate reductase (Frd) and aerobically expressed *E. coli* succinate dehydrogenase (Sdh) are structurally and functionally highly similar. They are therefore both included in the superfamily of complex II enzymes. Fumarate reductase, which functions as a terminal respiratory enzyme, oxidizes menaquinol to menaquinone and transfers its electrons to fumarate, reducing it to succinate. Succinate dehydrogenase, as part of the respiratory chain, catalyzes the opposite reaction and reduces ubiquinone to ubiquinol. Both enzymes are membrane-bound and are composed of four subunits: FrdA, B, C and D and SdhA, B, C and D. While FrdAB and SdhAB are very similar, the membrane-spanning hydrophobic subunits FrdCD and SdhCD – which anchor the FrdAB or SdhAB subunit to the membrane – are not. For example, SdhCD carries a b_{556} heme with uncertain function (indicated as '*b*' in figure 2) which is absent in FrdCD [8, 9, 10].

The FrdA and SdhA subunit both contain a covalently attached FAD moiety, which is involved in fumarate reduction/succinate oxidation. A 'capping domain' undergoes a conformational change when substrate is bound, closing the active site until the product, formed by hydride transfer from/to the FAD prosthetic group, is ready to be released [9, 11, 12, 13].

Finally, the FrdB and SdhB subunits, which contain three iron-sulfur clusters ($[2Fe\text{-}2S]^{2+,1+}$, $[4Fe\text{-}4S]^{2+,1+}$ and $[3Fe\text{-}4S]^{1+,0}$), relay electrons between the site of menaquinol oxidation/ubiquinone reduction and the FAD moiety. Although the potentials differ, the [4Fe-4S] cluster has an unexpectedly low redox potential in both enzymes, as compared to the two adjacent clusters (150-250 mV difference). This cluster nevertheless participates in the linear electron transport chain in FrdB and SdhB, despite its low redox potential. The proximity of the other two iron-sulfer clusters may provide an explanation. In this scenario, the edge-to-edge distance between the redox centers is a more determining factor in electron transfer, as compared to their midpoint potentials [14]. In addition, bond breaking and formation are often limiting to the overall catalytic rate of the enzyme, not the electron transfer rate [15, 16].

In this study, it was attempted to immobilize – or at least temporarily bind – *E. coli* succinate dehydrogenase and *E. coli* fumarate reductase to gold electrodes using appropriate Q-wires, which have been introduced in the previous chapters. Upon binding of the enzyme, a catalytic signal is expected to be observed in the presence of substrate, indicating a direct electronic connection between electrode and enzyme. Here, fully purified succinate dehydrogenase was used. Depending on the experiment, fumarate-reductase-enriched membranes, membrane extract or purified fumarate reductase was used.

5.1.2 *E. coli* cytochrome bo_3

The *E. coli* cytochrome bo_3 ubiquinol oxidase functions as the predominant terminal oxidase under aerobic circumstances [2]. This four-subunit membrane-bound oxidoreductase is a member of the superfamily of proton pumping heme-copper oxidases [17]. It accepts two electrons from ubiquinol-8, and utilizes them for the four-electron reduction of oxygen to water, while pumping four protons across the membrane, contributing to the proton electrochemical gradient. The largest subunit – subunit I – contains all redox centers: a heme *b* (‘*b*’ in figure 2); a heme o_3 (‘o_3’ in figure 2) and a copper ion (Cu_B) [18]. The latter two form the binuclear center where oxygen is bound and reduced, whereas heme *b* is involved in electron transfer to this binuclear center [19]. The enzyme has a low affinity (Q_L) and a high affinity (Q_H) site for binding ubiquinol-8. The Q_H-site binds ubiquinol-8 so tightly that the bound ubiquinol can be considered a cofactor. In this scenario, it is likely to be involved in electron transfer from the Q_L-site (which can then be considered the ‘normal’ active site for quinol oxidation during catalysis) to the heme *b*. Indeed, the semiquinone of the Q_H-bound quinol is stabilized by the enzyme, suggesting a role as ‘converter’ of two-electron to one-electron transfer [2].

E. coli cytochrome bo_3 was subjected to similar experiments as described for succinate dehydrogenase and fumarate reductase. In these experiments, fully purified His_6-tagged cytochrome bo_3 [20] was used.

5.1.3 *E. coli* DMSO reductase

Anaerobic respiratory growth of *E. coli* on media containing DMSO (dimethyl sulfoxide) is enabled by the trimeric membrane-bound menaquinol:DMSO oxidoreductase (DmsABC), where it functions as a terminal electron transfer complex [21]. Menaquinol provides the two electrons required for the reduction of DMSO to dimethyl sulfide (DMS) and water, which occurs at a catalytic site located in subunit DmsA, which contains a molybdopterin cofactor (indicated as 'Mo' in figure 2). Menaquinol oxidation is performed by a catalytic site located in DmsC, a subunit that additionally functions as the enzyme's membrane anchor. DmsB, an iron-sulfur protein, contains four [4Fe-4S] clusters, some of which are involved in electron transfer between DmsC and the catalytic site of DmsA [22-24].

Here, the experimental objective differs slightly from the ones stated above. No overexpressing strains, purified enzyme or enzyme-enriched membranes were used, but a 'wild type' membrane preparation was used instead, obtained from wild type *E. coli* (DH5α) grown anaerobically on a glycerol/DMSO minimal medium. The objective was to verify whether the aforementioned system would be suitable for performing electo-enzymology directly on unpurified membranes, containing only relatively low enzyme concentrations. In this scenrario, the Q-wires would selectively 'plug into' the enzyme of interest. If successful, no overexpression strain construction or protein purification would be necessary, greatly simplifying the experiment.

5.1.4 Towards protein film voltammetry

In protein film voltammetry (PFV), a redox enzyme of interest is immobilized as a stable (sub)monolayer on the surface of an electrode. Ideally, the electrode provides the enzyme with electrons directly in a non-rate-limiting fashion, eliminating the need for a mediator that shuttles electrons between electrode and enzyme. This removes the problems associated with slow diffusion and kinetics, simplifying data analysis. Further benefits include the possibility of fast screening under different

(and extreme) circumstances: the modified electrode can be shortly exposed to different solutions of e.g. different (and extreme) pH. In addition, since only a (sub)monolayer of enzyme is required, very small amounts of protein are needed [25].

Fully immobilized, stable (sub)monolayers of redox enzyme were not achieved using the system presented in figure 1, yet fruitful electron transfer between the Q-wires and enzymes was nevertheless observed, especially in case of succinate dehydrogenase. Although the presence of alkanethiols on the electrode surface may have stabilized the protein 'film' through hydrophobic interactions, further modifications are required to achieve a stable, immobilized film. Only then can be profited from all the advantages pertaining to protein film voltammetry.

5.2 Results and discussion

In this section, the results from a series of cyclic voltammetry experiments are presented. These experiments were performed using electrodes decorated with a Q-wire and an alkanethiol co-SAM, as exemplified by figure 1. The Q-wires relay electrons between enzyme and electrode, which, in the presence of substrate, allows for the measurement of catalytic currents.

As will be seen below, the catalytic currents due to enzyme activity are generally relatively small compared to the quinone reduction and oxidation peaks, and separation of the signals can therefore be challenging. One obvious way to circumvent this problem is to limit the electrode surface coverage of the Q-wire. Another strategy exploits the considerable hysteresis between the oxidation and reduction peaks of the longer Q-wires at approximately neutral pH. For example, while performing cyclic voltammetry with no enzyme present, by simply reversing the potential scanning direction before the reduction peak of the quinone is reached, the quinone is kept oxidized, and the oxidation peak therefore disappears. If enzyme (e.g. succinate dehydrogenase) is then added and its catalytic activity (e.g. succinate oxidation) results in the reduction of the quinone moiety, the measured anodic current is entirely attributable to enzyme

activity. The reverse is also true for enzymes oxidizing the quinol (e.g. fumarate reductase), where the potential scan window should exclude the oxidation region of the quinol, keeping it reduced. In conclusion, by 'silencing' the reduction and oxidation peaks of the Q-wire, the catalytic current can be isolated.

Besides relatively small catalytic currents, which complicate performing meaningful electro-enzymology, an additional obstacle was encountered. Although a standardized protocol was used for the preparation of the working electrodes, the measured enzyme activities obtained from identical experiments varied widely. Because these variations were unlikely due to improper enzyme treatment or buffer conditions, irregularities at the working electrode surface (e.g. composition, topology, contaminations, etc) are the most likely causes. To address this poor reproducibility, thorough optimization of the working electrode treatment (and subsequent enzyme interactions) is still required for quantitative investigations and applications.

Another, more fundamental and – in some cases – perhaps insurmountable problem lies in obtaining a correct background current. The measured current can be corrected using a suitable background current to reveal the catalytic current due to enzymatic activity. Although most experiments were started by recording voltammograms prior to addition of enzyme to the electrolyte, these data usually cannot be used as 'blank', since the addition of an enzyme preparation (notably including surfactant or membrane fragments) by itself influences the background current. When enzymatic activity is present, the background current is essentially unknown. In the experiments described below, enzyme inhibitors proved useful in some cases. In this scenario, enzyme activity is inhibited, removing the catalytic current and revealing the background current. However, inhibition may be incomplete or the inhibitors may have additional effects on the measured current. This is especially true for e.g. potassium cyanide, used to inhibit cytochrome bo_3 activity, which was observed to interact with the gold electrode surface, influencing the measured current. To prevent the latter, the electrode surfaces were decorated with dense(r) co-SAMs of

heptanethiol. An additional benefit to this strategy lies in the minimization of nonspecific oxygen reduction by the electrode surface.

The complications described above clearly limit the extent to which enzyme activity can be quantified using the aforementioned system. Therefore, in order to be able to perform meaningful, quantitative electro-enzymology, it still has to undergo substantial optimization.

5.2.1 Succinate dehydrogenase electro-enzymology

As can be appreciated in figure 3, which depicts cyclic voltammograms of an electrode modified as shown in figure 1 (**U_3** SAM and heptanethiol as co-SAM) before and after addition of succinate dehydrogenase, only minor differences can be detected that can be attributed to enzyme activity. While recording, enzyme addition causes the ubiquinol oxidation peak to gradually shift towards lower potentials; a subtle but consistently observed effect. As mentioned above, catalytic currents due to enzyme activity are generally relatively small compared to the quinone reduction and oxidation peaks. Therefore, in order to obtain meaningful enzymological information, another approach must be considered.

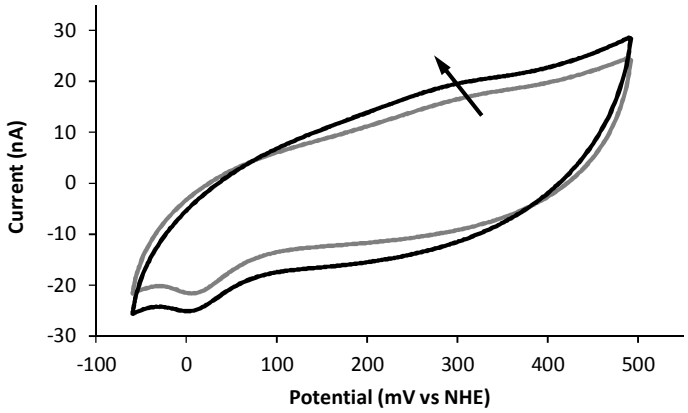

Figure 3 Catalytic voltammograms of *E. coli* succinate dehydrogenase (purified); buffer: 50 mM MOPS pH 7.2, 5 mM EDTA, 50 mM succinate, 0.005% lauryl maltoside, 20°C; scan rate: 5 mV/s; electrode modifications: **U_3** and heptanethiol. The arrow indicates the development of the anodic peak over 15 scans

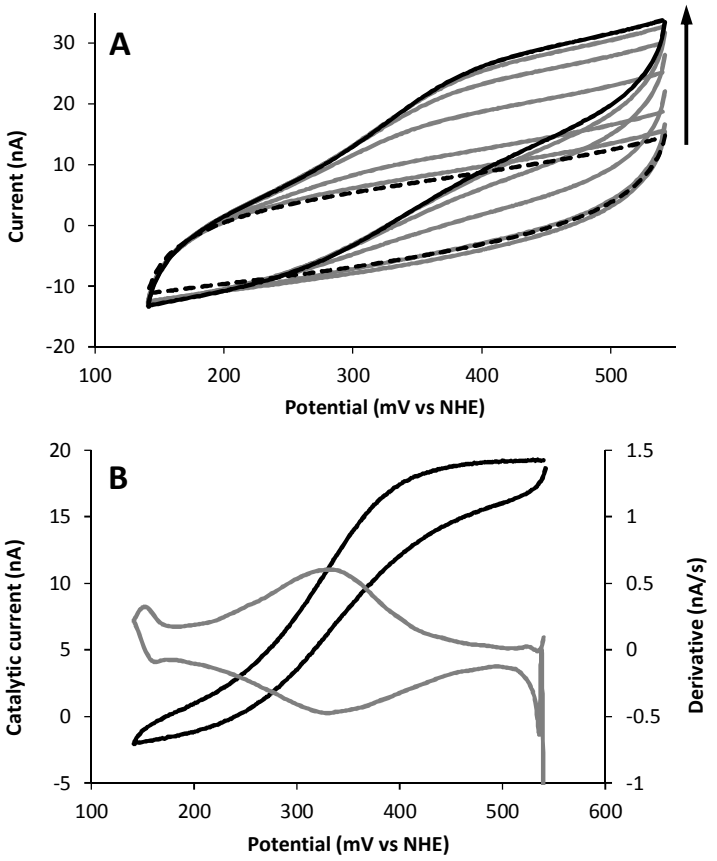

Figure 4 (A) Catalytic voltammograms of *E. coli* succinate dehydrogenase (purified); buffer: 50 mM MOPS pH 7.2, 5 mM EDTA, 50 mM succinate, 0.005% lauryl maltoside, 20°C; scan rate: 5 mV/s; electrode modifications: $\mathbf{U_{SAT}}$ and heptanethiol. The arrow indicates the development of the catalytic signal over 17 scans (B) Catalytic current (final minus first scan in A; black line) and its derivative (gray line)

Here, it was attempted to 'silence' the quinol peaks by restricting the potential scanning window, as can be observed in figure 4A ($\mathbf{U_{SAT}}$ SAM and heptanethiol co-SAM). After addition of enzyme and in the presence of succinate, a catalytic wave gradually builds up and then stabilizes. Although not shown here, after a period of stable enzymatic catalysis, gradual inactivation was often observed. As expected, a sigmoidal curve, which is characteristic of a catalytic process, is obtained (figure 4B, black line) when

the measured wave (figure 4A, solid black line) is corrected for the background current (figure 4A, dashed black line). The derivative (figure 4B, gray line) reveals a peak above 300 mV vs NHE in both the oxidation and reduction direction.

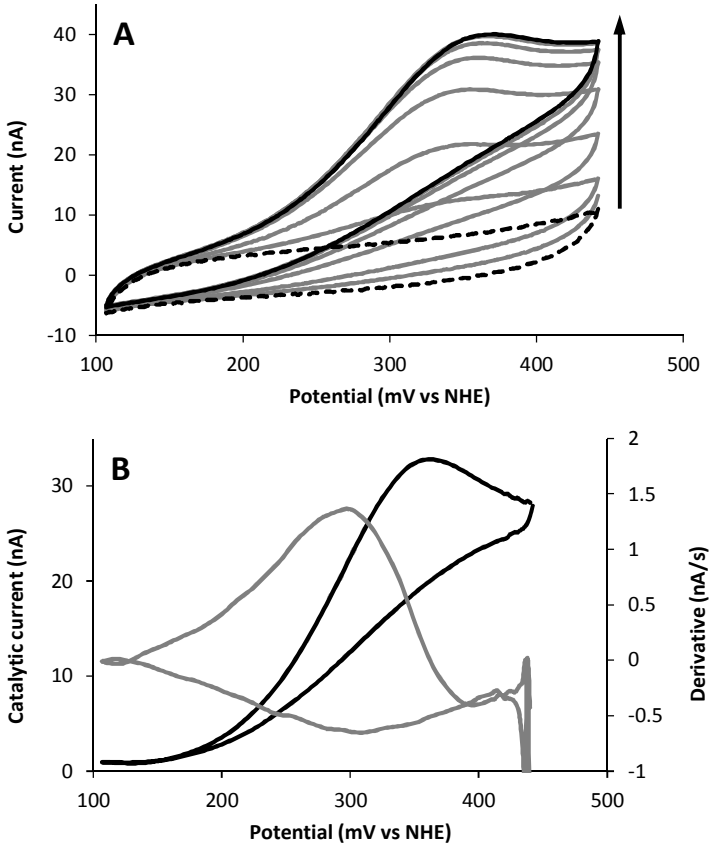

Figure 5 (A) Catalytic voltammograms of *E. coli* succinate dehydrogenase (purified); buffer: 50 mM MOPS pH 7.2, 5 mM EDTA, 50 mM succinate, 0.005% lauryl maltoside, 20°C; scan rate: 5 mV/s; electrode modifications: $\mathbf{U_3}$ and heptanethiol. The arrow indicates the development of the catalytic signal over 13 scans (B) Catalytic current (final minus first scan in A; black line) and its derivative (gray line)

Figure 5 represents a similar set of data obtained from an electrode modified with $\mathbf{U_3}$. Here, at potentials above 360 mV (the activity maximum, which was not observed for the other wires), the enzyme activity decreases

somewhat (figure 5B, black line), possibly due to mass transport limitations (e.g. local depletion of substrate, which could imply faster electron transfer for $\mathbf{U_3}$ in comparison to $\mathbf{U_{SAT}}$). Although less symmetrical, the derivative depicted in figure 5B (gray line), again shows peaks around 300 mV vs NHE. It should be noted that these values vary between experiments, but usually appear at higher potentials in comparison with the ubiquinol oxidation peak in absence of enzyme, implying the need of an overpotential when enzymatically oxidizing succinate. However, this potential shift may reflect a change in pK_a or $E^{0'}$ of the quinone moiety, which occurs when it enters the enzyme's active site.

An explanation for the slowly increasing signals, observed in figures 4A and 5A and summarized in figure 6, could lie in the binding and diffusion kinetics of the enzyme to the wires. The electrode surface topology or contaminants on or near the electrode surface (e.g. micelles of lauryl maltoside or denatured protein) may perhaps limit said diffusion and binding, prohibiting a rapidly developing signal. Such irregularities may also have caused the observed variability in the measured enzyme activities, hindering reproducibility and quantification. Another explanation may simply be that the enzyme undergoes slow activation during the measurements. Indeed, some protocols describe the activation of succinate dehydrogenase prior to experimentation [26].

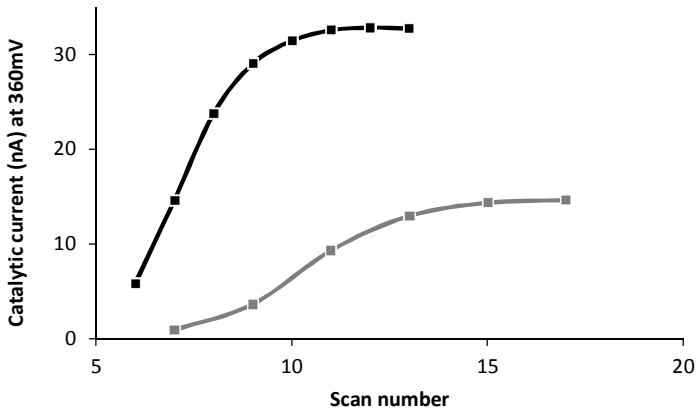

Figure 6 Development of succinate dehydrogenase activity, measured as catalytic current at 360 mV, when using $\mathbf{U_{SAT}}$ (gray) or $\mathbf{U_3}$ (black) as electode decoration

Oxaloacetic acid is a potent inhibitor of succinate dehydrogenase [27], and, in addition, does not appear to disturb the background current while performing cyclic voltammetry. It was therefore used in a set of experiments in which all ubiquinone-terminated wires ($\mathbf{U_0}$-$\mathbf{U_3}$ and $\mathbf{U_{SAT}}$) were subjected to activity and inhibition studies. Figure 7 exemplifies these inhibition studies. Figure 7A illustrates the aforementioned 'silencing' of the ubiquinone peaks by limiting the potential scan range.

As can be concluded from the results presented in appendix 1-5, there is a considerable variability in the observed enzyme activities – even when the experiments were performed identically. Although it is tempting to conclude that $\mathbf{U_0}$ and $\mathbf{U_1}$ – considering the low enzyme activities and required overpotentials – are the least suitable wires for the type of experiment presented here, the importance of the aforementioned variability must be emphasized and therefore much larger datasets are required to be able to draw a definitive conclusion. Should further measurements be consistent with the above data, a straightforward explanation may then lie in the shorter length of these wires. In this scenario, the wires are either insufficiently long to reach the active site of the enzyme or to penetrate a layer of contaminations associated with the electrode surface. Indeed, the catalytic current observed for $\mathbf{U_0}$ does not appear to be much more substantial in comparison with the (nonspecific) 'catalytic' current observed for a 'blank' electrode (no wire, heptanethiol SAM).

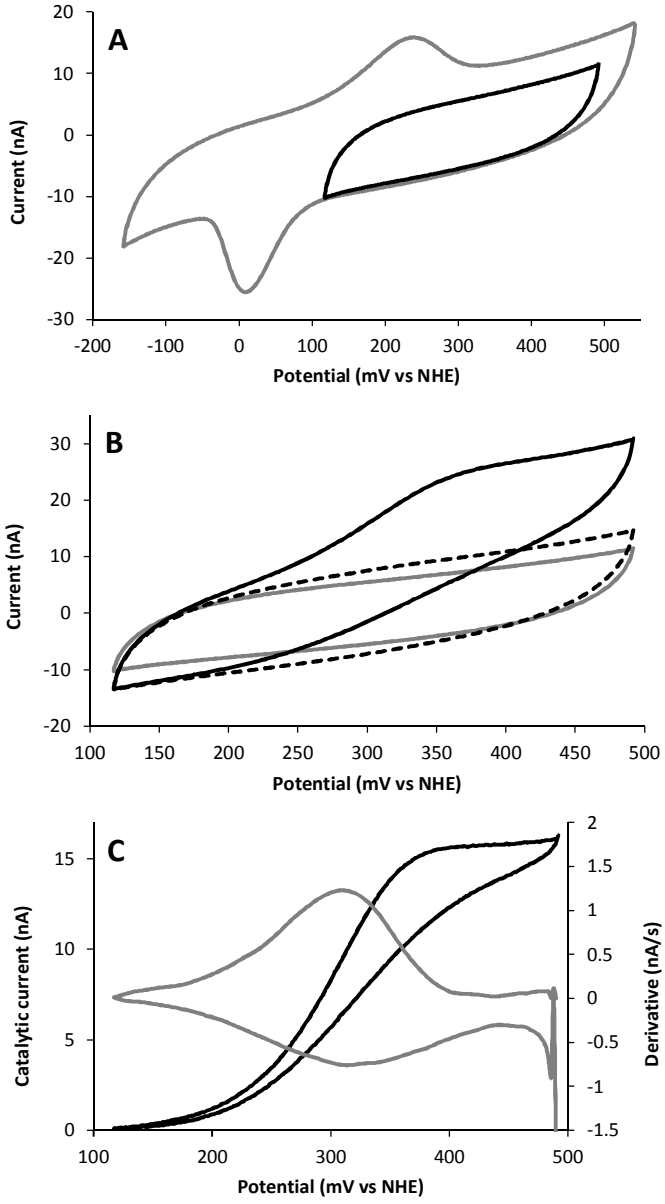

Figure 7 (A) Cyclic voltammograms of a $\mathbf{U_2}$- and heptanethiol-modified electrode at different potential ranges in 50 mM MOPS pH 7.2, 5 mM EDTA, 50 mM succinate, 20°C; scan rate: 10 mV/s (B) Catalytic voltammogram after addition of *E. coli* succinate dehydrogenase (black solid line; before addition: gray line); inhibited signal after addition of oxaloacetic acid (40 mM; black dashed line) (C) Catalytic current (solid minus dashed black line in B) and its derivative (gray line)

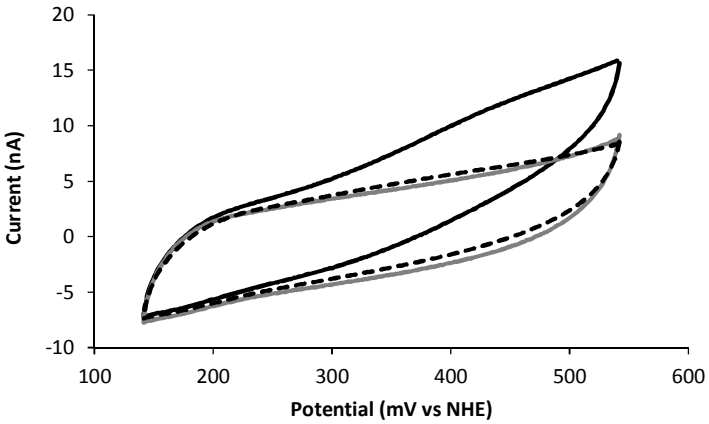

Figure 8 Effect of washing a $\mathbf{U_3}$- and heptanethiol-modified electrode after measuring *E. coli* succinate dehydrogenase activity; buffer: 50 mM MOPS pH 7.2, 5 mM EDTA, 50 mM succinate, 20°C; scan rate: 5 mV/s. Gray line: before addition of enzyme; black solid line: after addition of enzyme and subsequent signal build-up; black dashed line: after washing with buffer

Another important question to be addressed was whether the wires were capable of immobilizing the enzyme by themselves, thereby forming a stable protein film on the electrode surface. As can be concluded from figure 8, this does not appear to be the case. Once stable enzyme activity was established, the measurement was halted and the buffer was removed. The electrode surface was then carefully rinsed with buffer (containing substrate, but no detergent) and the buffer droplet was replaced, after which scanning was continued. However, no significant residual activity was found, suggesting no stable protein film of active enzyme was present on the electrode surface. Moreover, addition of fresh enzyme to the droplet did not lead to the reestablishment of the catalytic signal (*data not shown*), which could indicate that the electrode surface had become inaccessible to the enzyme, perhaps due to the presence of an impenetrable layer of contaminants (detergent, denatured protein, etc) on the electrode surface. Therefore, no definitive conclusion regarding the binding strength between the enzymes and the wires can be drawn, since the enzyme activity may have been compromised due to the washing treatment. Some possible strategies that may eventually lead to more stable protein films have been discussed in chapter 2.

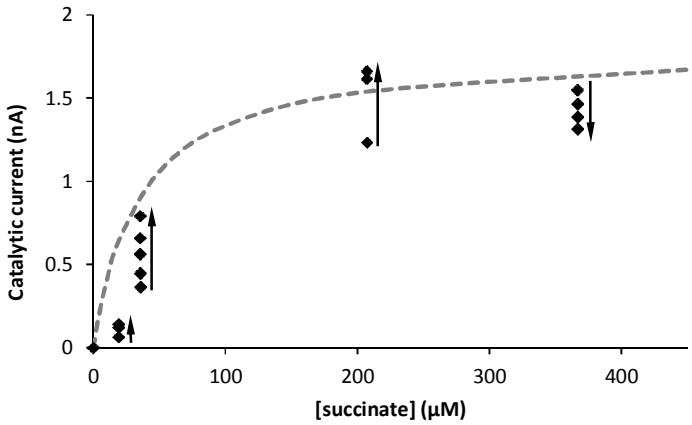

Figure 9 Catalytic current of *E. coli* succinate dehydrogenase measured at different substrate concentrations on a $\mathbf{U_0}$- and heptanethiol-modified electrode in 50 mM MOPS pH 7.2, 5 mM EDTA, 0.005% lauryl maltoside, 20°C; scan speed: 5 mV/s. The buffer droplet was titrated with a concentrated succinate solution to achieve the desired concentration. The arrows indicate the development of the catalytic signal over time. Gray dashed line: Michaelis-Menten plot, using I_{max} = 1.8 nA and K_M = 35 µM)

As mentioned above, enzyme activity varied substantially among different electrodes, making further enzymological experimentation, e.g. a basic Michaelis-Menten kinetic analysis, challenging. Here, however, the need for several differently behaving electrodes was circumvented by using a single electrode and by titrating the buffer droplet – already containing enzyme – with succinate, thereby hopefully obtaining a substrate saturation plot. While reminiscent of such a plot (gray dashed line), when inspecting figure 9, however, it becomes clear that the data are a convolution of substrate saturation, gradual enzyme activation and enzyme inactivation, limiting the usefulness of these data. Superficial analysis (using only the highest currents per substrate concentration) suggests an apparent K_M value of around 35 µM for succinate, which is higher than the previously reported K_M of 20 µM [28].

Perhaps a more robust approach may lie in the use of a dedicated electrode for each substrate concentration to be measured. In this scenario, after a stable enzyme activity has been achieved, excess substrate is added to the droplet in order to measure the maximum activity. The former

measurement is then normalized using the latter, hopefully producing a statistically more reliable, relative (dimensionless) enzyme activity that can be used in e.g. Michaelis-Menten analysis.

As mentioned previously, irregularities at the working electrode surface (contaminations, differing electrode topology, etc.) hinder reproducibility and quantitative measurements. However, based on the geometric properties of the electrode surface and the enzyme, it is possible to roughly estimate a lower limit of the 'catalytic rate constant k_{enz}', which is here defined as the number of electrons exchanged between enzyme and electrode per second. For example, a (maximum) catalytic current $i_{cat} \approx 32$ nA (see figure 5B) suggests a lower limit of $k_{enz} \geq 3\ s^{-1}$ (for calculation and assumptions, see experimental section) for a perfectly assembled full monolayer of functional enzyme (i.e. not denatured) on a smooth electrode surface, in which every enzyme has access to at least one Q-wire. Because the conditions at the electrode surface are unlikely to be this ideal, the obtained value for k_{enz} is likely to be a significant underestimation. If the observed activity is comparable to the succinate-ubiquinone-1 reductase activity described elsewhere ($k_{cat} = ½k_{enz} = 78s^{-1}$, 30°C, pH 7.8 [29]), k_{enz} lies within the domain $\sim 3\ s^{-1} < k_{enz} < \sim 150\ s^{-1}$, which is much higher in comparison with the apparent electron transfer rate constant k_{app} measured in buffer, as described in chapter 4 ($k_{app} = 0.012\ s^{-1}$, 50 mM MOPS pH 7.2, I = 0.5; identical electrode modifications). This suggests that k_{app} is limited by (de)protonation rates, and that the enzyme catalyzes said (de)protonations. Based on the information presented here, however, it is still inconclusive whether the Q-wires facilitate non-rate-limiting electron transfer – as was claimed in the preceding text. Perhaps the apparent substrate depletion observed in figure 5B confirms that the measured catalytic activity is limited by substrate diffusion and not by electron transfer by the Q-wires, justifying the claim.

5.2.2 Fumarate reductase electro-enzymology

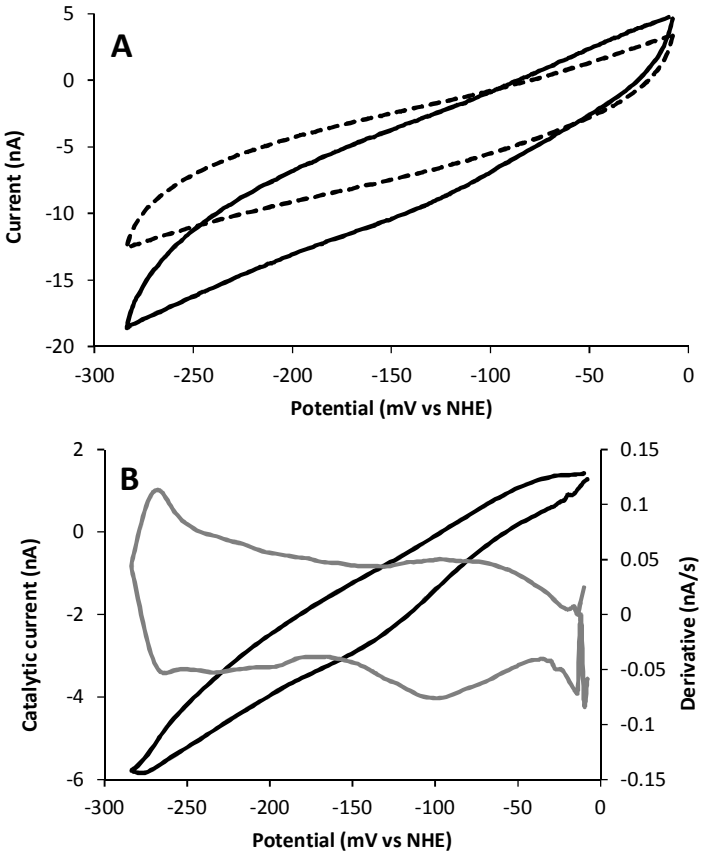

Figure 10 (A) Catalytic voltammograms of *E. coli* fumarate reductase (enriched membrane suspension) before (solid line) and after inhibition with $ZnSO_4$ (16 mM; dashed line); buffer: 50 mM MOPS pH 7.2, 5 mM EDTA, 100 mM fumarate, 20°C; scan rate: 2 mV/s; electrode modifications: $\mathbf{M_3}$ and heptanethiol (B) Catalytic current (solid minus dashed line in A) and its derivative (gray line)

Because of the similarity between succinate dehydrogenase and fumarate reductase, comparable behavior may be expected in the experiments performed in this study (in which menaquinone-terminated wires were used instead). In general, however, lower activity was observed (figure 10 – fumarate reductase enriched membranes; $\mathbf{M_3}$-decorated electrode). By addition of zinc sulfate – which was found to be a suitable inhibitor for this enzyme – to the reaction droplet, a baseline was obtained, which was then

subtracted from the voltammograms showing enzymatic activity. Indeed, the resulting curve (figure 10B, black line) resembles the expected sigmoidal shape and its derivative shows a clear peak around -100 mV vs NHE in the reductive direction.

Some efforts (see appendix 6) were made to improve the enzyme's activity and stability. The latter was limited to only a few scans, considerably lower in comparison with succinate dehydrogenase. Several different co-SAMs were considered, including 3-mercaptopropionic acid, alkanethiols of different length and 6-mercaptohexanol, none of which led to an appreciable enhancement of the enzyme's activity or stability. In addition – while in most experiments fumarate reductase enriched membranes were used – it was assessed whether membrane extraction and/or full purification would enhance the enzyme's performance. However, no noticeable improvements were detected. On the contrary, full purification appeared to be detrimental to the enzyme's stability. Here, after a brief period of activation, inactivation became predominant and enzyme activity was abolished.

5.2.3 Cytochrome *bo*$_3$ electro-enzymology

As mentioned previously, when enzymatic activity is present, the background current is essentially unknown. By inhibiting the enzyme, one may obtain a suitable background current, but only when the concerning inhibitor does not have additional effects on the measured current. However, potassium cyanide, which was used here, does (under aerobic conditions). To prevent its interaction with the gold electrode surface, the surfaces were decorated with dense(r) co-SAMs of heptanethiol. Additionally, this strategy minimizes nonspecific oxygen reduction by the electrode surface, which is a complication because it distorts the catalytic signal. Moreover, nonspecific oxygen reduction may be in competition with the enzyme for oxygen, causing an increase in background current after enzyme inhibition. Furthermore, interactions between the gold electrode surface and enzyme inhibitors may have an effect on the nonspecific oxygen reduction, complicating the interpretation of the background current even further.

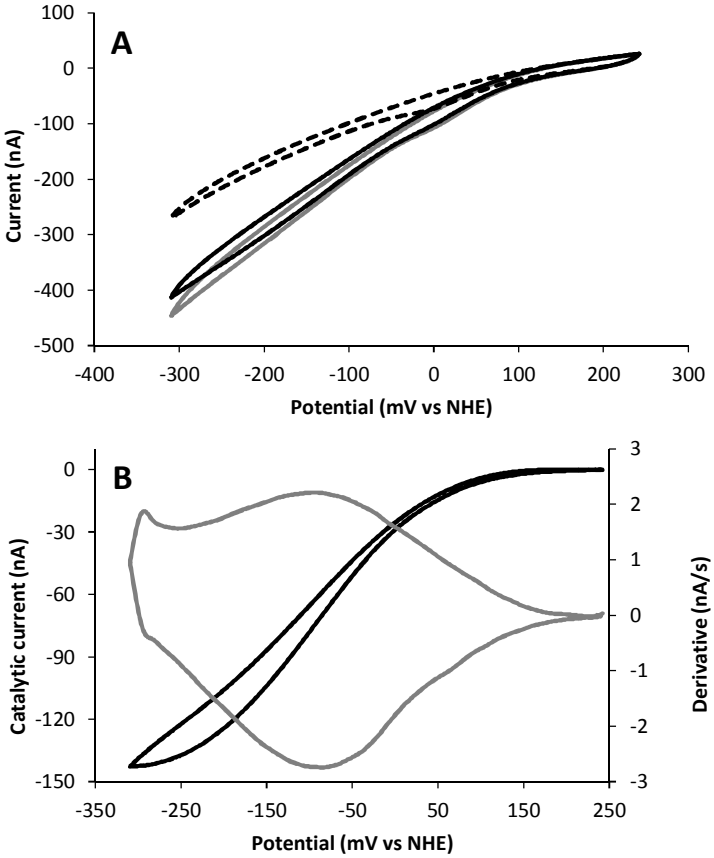

Figure 11 (A) Catalytic voltammograms of *E. coli* cytochrome bo_3 (purified) before (solid black line) and after inhibition with KCN (100 µM; dashed line); gray line: before addition of enzyme; buffer: 50 mM MOPS pH 7.2, 5 mM EDTA, lauryl maltoside, 20°C; scan rate: 5 mV/s; electrode modifications: $\mathbf{U_3}$ and heptanethiol (B) Catalytic current (solid black line minus dashed line in A) and its derivative (gray line)

As can be observed in figure 11A, addition of enzyme appears to have little influence on the cathodic current, possibly because the (partially denatured) enzyme and detergents further prevent nonspecific oxygen reduction by the electrode surface. The subsequent addition of potassium cyanide removes the current due to enzymatic activity, whereby the remaining background current is revealed. This is then used to correct the measured 'uninhibited' current, producing the expected sigmoidal curve (figure 11B, black line), presumably representing enzymatic activity. In the

reductive direction, the derivative (figure 11B, gray line) shows a peak around -100 mV, a value also found for a $\mathbf{U_{SAT}}$-modified electrode (see appendix 7). In case of a 'blank' electrode (heptanethiol SAM only) the corresponding peak was found at approximately -35 mV (figure 12B, gray line). Note that the latter peak is broader than the former, suggesting a more heterogeneous electron transfer distribution for wire-independent catalysis. It must be stressed that, although the blank shows only little (apparent) catalytic activity, results may vary widely among experiments.

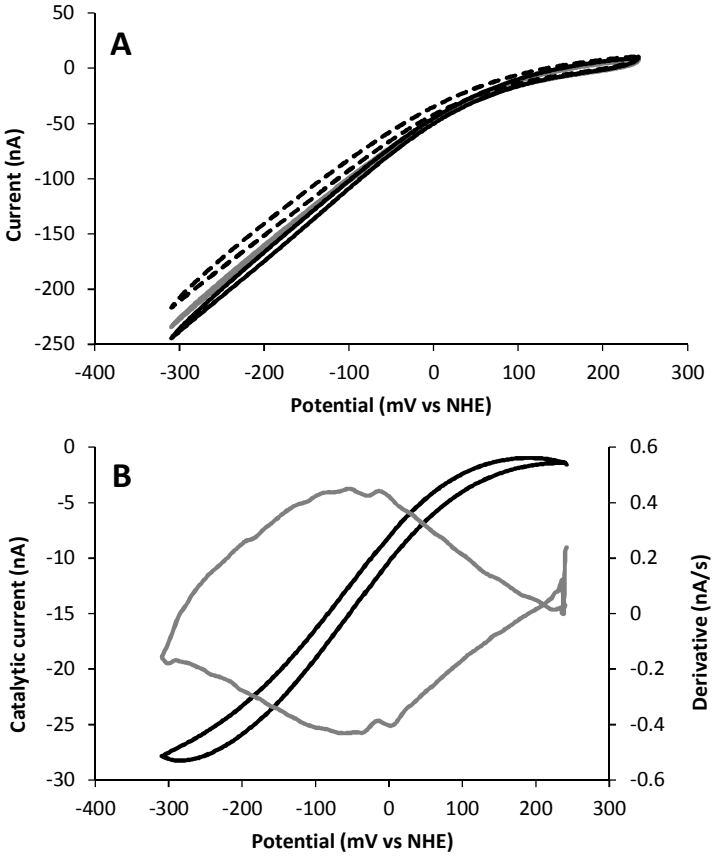

Figure 12 (A) Voltammograms of *E. coli* cytochrome bo_3 (purified) on a heptanethiol-modified electrode before (solid black line) and after inhibition with KCN (100 µM; dashed line), suggesting some wire-independent enzymatic activity; gray line: before addition of enzyme; buffer: 50 mM MOPS pH 7.2, 5 mM EDTA, lauryl maltoside, 20°C; scan rate: 5 mV/s (B) Apparent catalytic current (solid black line minus dashed line in A) and its derivative (gray line)

It becomes evident that the measured currents are a convolution of many different processes. These factors include: nonspecific oxygen reduction by the electrode; effects of potassium cyanide on the current; condition of the electrode surface (contamination); wire-assisted enzymatic activity and wire-independent enzymatic activity. Although observed (figure 12), the origin (or existence) of the latter factor is unknown. Perhaps direct electron transfer from the electrode to the enzyme is possible to a degree, independent of the Q-wires. This may be reflected by the different midpoint potentials found for Q-wire mediated (-100 mV) and wire-independent catalysis (-35 mV).

In conclusion, experiments involving cytochrome bo_3 suffer from a number of additional complications, such as the unknown origin of the – apparently enzymatic – wire-independent activity and the unknown influence of potassium cyanide on the electrode, making reliable quantification even more challenging. However, when zinc sulfate was used as inhibitor, comparable results were obtained (figure 13). In fact, the cathodic current could be restored by addition of an excess of the chelator EDTA. The similarity between the results suggests that potassium cyanide may still be a useful inhibitor in these experiments – provided that the gold electrode surface is sufficiently covered by thiols – and that the difference between the 'uninhibited' and 'inhibited' current indeed represents enzymatic activity.

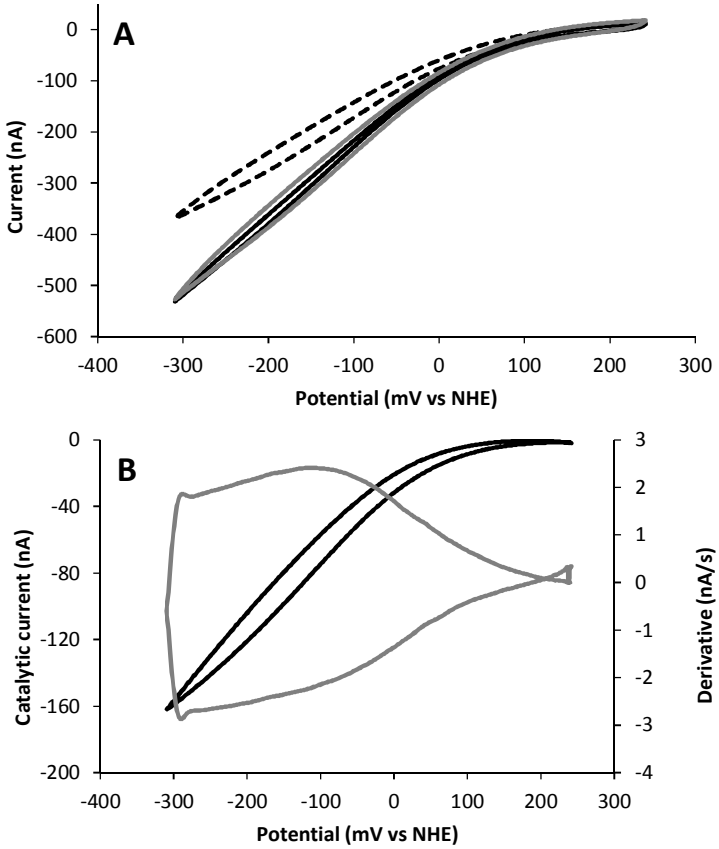

Figure 13 (A) Catalytic voltammograms of *E. coli* cytochrome bo_3 (purified) before (solid black line) and after inhibition with $ZnSO_4$ (8 mM; dashed line); gray line: reconstitution of enzyme activity by addition of sat. EDTA; buffer: 50 mM MOPS pH 7.2, 5 mM EDTA, lauryl maltoside, 20°C; scan rate: 5 mV/s; electrode modifications: $\mathbf{U_3}$ and heptanethiol (B) Catalytic current (solid black line minus dashed line in A) and its derivative (gray line)

5.2.4 DMSO reductase electro-enzymology on wild-type membranes

Finally, in the experiments presented here, a 'wild type' cytoplasmic membrane preparation, obtained from wild type *E. coli* (DH5α) grown anaerobically on a glycerol/DMSO minimal medium, was used. It was verified whether the system introduced in this chapter could be used to perform enzymological meaningful experiments on easily obtained wild type membranes, containing only a relatively low amount of DMSO

reductase. If successful, sample preparation would be greatly simplified, requiring no complex purification.

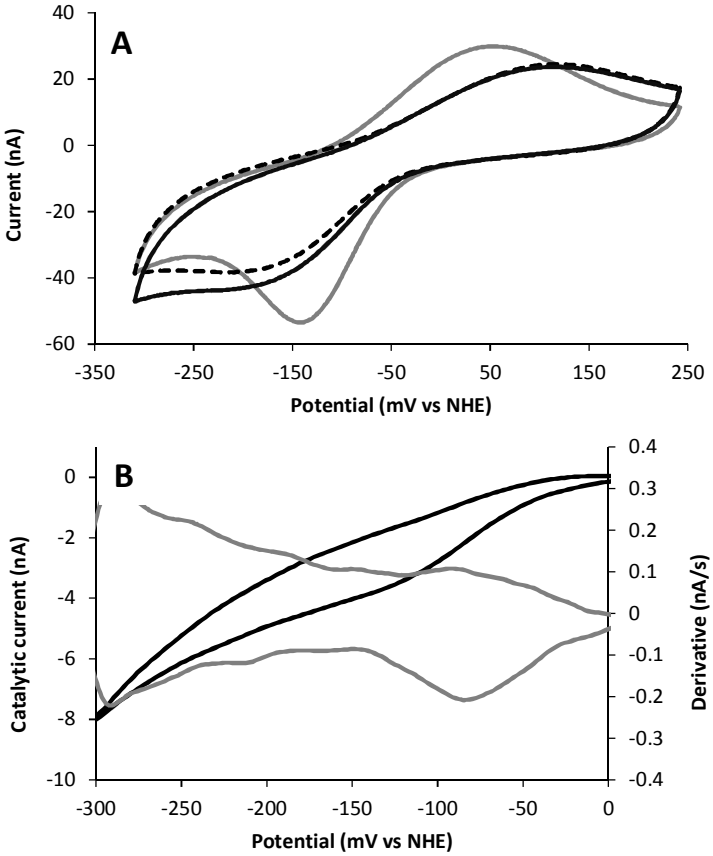

Figure 14 (A) Catalytic voltammograms of *E. coli* DMSO reductase (membrane preparation) before (solid black line) and after inhibition with HQNO (0.4 mM; dashed line); gray line: before addition of enzyme; buffer: 200 mM potassium phosphate pH 6.8, 1 mM EDTA, 25 mM DMSO, 20°C; scan rate: 5 mV/s; electrode modifications: $\mathbf{M_3}$ and heptanethiol (B) Catalytic current (solid black line minus dashed line in A) and its derivative (gray line)

As observed previously, addition of enzyme (here: wild type membranes) profoundly alters the wave form of the voltammogram (figure 14A, solid black line); the peaks associated with $\mathbf{M_3}$, with which the concerning electrode is modified, become less pronounced and appear more sigmoidal. When HQNO – a potent inhibitor of quinol oxidases [2, 30, 31] – is

subsequently added, the wave shape associated with the cathodic current changes. When subtracted from the voltammogram presumably featuring enzymatic steady state activity, a curve reminiscent of a sigmoid is revealed (figure 14B, black line). The derivative (fig 14B, gray line) of the latter curve shows a clear peak at -85 mV vs NHE.

Although the results presented above suggest that enzymatic activity indeed can be detected in unpurified, wild-type membranes, the relatively small observed currents and poor reproducibility likely complicate meaningful enzymological experimentation, as was concluded before.

5.3 Conclusion & outlook

Especially in case of succinate dehydrogenase, convincing catalytic currents were observed, facilitated by Q-wires. Based on the results presented in this chapter, it can be concluded that both ubiquinone- and menaquinone-terminated Q-wires are capable of successfully establishing an electron transfer pathway between electrode and enzyme. Although it is not yet clear whether this electron transfer is indeed non-rate-limiting, estimations of electron transfer rate constants (k_{enz}) found in this chapter were orders of magnitude greater in comparison with the rate constants (k_{app}) encountered in the previous chapter, suggesting much faster electron transfer through enzyme-bound Q-wires. Further experimental optimizations should provide a more quantitative answer as to what electron transfer rates can be achieved by enzyme-bound Q-wires, and whether they are rate-limiting.

Nevertheless, a considerable number of issues were encountered while performing the experiments presented in this chapter. Usually, only small catalytic currents attributable to enzyme activity were measured, complicating their separation from the background current. Indeed, suitable background currents – required to obtain the enzymatic signal – were frequently not available and in some cases, e.g. in case of cytochrome bo_3, even questionable. Moreover, the variability in the measured catalytic currents among identically performed experiments impeded performing meaningful electro-enzymology.

As mentioned before, the most likely explanation for most of the issues described above are irregularities at the working electrode surface (e.g. composition, topology, contaminations, etc). To address the aforementioned poor reproducibility of the experiments, thorough optimization of the working electrode treatment (and subsequent enzyme interactions) is still required.

The formation of stable, immobilized protein films was not achieved in the experiments described above. Therefore, in order to benefit from the advantages associated with protein film voltammetry, further electrode surface (or protein) modifications are still required. It may be possible, for example, to anchor fragments of the cytoplasmic membrane, containing a redox enzyme of interest, to the electrode, as has been described before [32]. In this scenario, in order to avoid the use of slowly diffusing mediators, the Q-wires relay electrons between enzyme and electrode.

As can be concluded from the experiments presented above, both menaquinone- and ubiquinone-terminated Q-wires are capable of providing electron transfer between electrode and enzymes, allowing for qualitative experimentation. However, in order to achieve the ultimate objective – assembling a stable enzyme monolayer on an electrode surface suitable for protein film voltammetry, in which the Q-wires provide non-rate-limiting electron transfer between electrode and enzyme – substantial optimization and innovation is still necessary.

5.4 Experimental

5.4.1 Electrochemistry

Working electrodes (2 mm diameter gold working electrode, CH-Instruments) were prepared in an identical manner as described in chapter 4. After polishing, the electrodes were decorated with the appropriate Q-wire (**U_0-U_3**, **U_{SAT}**, or **M_0-M_3**) by incubation in the corresponding 'deprotection mixture' until the desired coverage was achieved. However, both the incubation time with (up to 30-60 mins) and concentration of the co-SAM (1% (v/v) in ethanol of either heptanethiol or propanethiol) were

increased, which was especially important for experiments not performed under argon. The electrodes were then installed in a 'Hagen cell' [33] and – where required – the cell was flushed with argon (or any oxygen/argon mixture), after first suspending a 25 µl droplet of buffer (in most cases 50 mM MOPS, pH 7.2, 5 mM EDTA, and – depending on the experiment – already containing substrate or enzyme) from the reference electrode (saturated KCl/calomel with porous glass junction, Radiometer REF401). At the start of a typical electro-enzymology experiment, the working electrode and the counter electrode (platinum wire) were brought in contact with the hanging droplet, after which the Q-wire coverage on the working electrode was assessed by means of cyclic voltammetry (staircase voltammetry (α= 1); step size 2 mV; usally at 50 mV/s, using an appropriate potential window). Scanning speeds were then lowered (2-10 mV/s) and potential windows were adjusted. Depending on the experiment, background voltammograms were recorded, (additional) enzyme and/or substrate (or v.v.) was injected into the buffer droplet, and an appropriate enzyme inhibitor was added, concluding the experiment. Further details on the experimental setup can be found in chapter 4.

5.4.2 *E. coli* succinate dehydrogenase

Purified E. coli succinate dehydrogenase was a gift from dr. G. Cecchini (Department of Biochemistry & Biophysics, University of California) and provided by prof. dr. S. de Vries (Delft University of Technology). The sample (430 µM) was diluted (100mM HEPES, pH8, 5mM EDTA, 0.1% lauryl maltoside), centrifuged (5 min, max. speed, 4°C, Eppendorf Centrifuge 5415D) and the supernatant was divided into portions, flash frozen using liquid nitrogen and stored at -80°C until use.

5.4.3 Expression and purification of *E. coli* fumarate reductase

The expression strain and membrane granules were produced during an internship at Delft University of Technology under the supervision of prof. dr. Simon de Vries [34]. The *frdABCD* operon was amplified from genomic DNA (*E. coli* K12) by means of PCR (forward primer: 5'-AAC GCA AGA AAG CTT GTT GAT AAG-3' (HindIII); reverse primer: 5'-TTC CCC TCG AGC AAT

AGC GTC-3' (XhoI)) and cloned into the low-copy vector pACYC177. Competent *E. coli* MC4100 cells were transformed with this construct and were subsequently grown on glycerol/fumarate minimal medium [35] supplemented with ampicillin (30 µg/ml) for ~40 hrs. Cells were harvested (10 min, 7000 rpm, 4°C, Sorvall RC-5B centrifuge, SLA-3000 rotor) washed (200 mM Tris HCl, pH 8.0) and disrupted (1.8 kbar, 'multi-shot' mode, LA Biosystems B.V., Waalwijk disruptor), after which cell debris was removed (15 min, 7000 rpm). Ultracentrifugation (1 hr, 40000 rpm, 4°C, Beckman OptimaTM L (45 Ti rotor)) yielded the desired membranes, which were then resuspended (25 mM MOPS-KOH, pH 7.2, 1 mM EDTA) in a minimal volume and subsequently flash frozen by drop-wise addition to liquid nitrogen. The resulting granules were stored at -80°C and some were used without further purification for certain electrochemistry experiments.

Some electrochemistry experiments were performed with membrane extracts or purified protein. Membrane extracts were obtained by resuspension of a few frozen membrane granules in ~1 mL buffer (50 mM MOPS, pH 7.2, 5 mM EDTA, 1% lauryl maltoside), which was then centrifuged (1-2 hrs, max. speed, 4°C, Eppendorf Centrifuge 5415D). The supernatant was then either concentrated (Amicon Ultra-0.5 mL Centrifugal Filter) and used for experiments, or subjected to further purification by chromatography (5 mL HiTrap DEAE Sepharose FF, GE Healthcare Life Sciences, buffer: 50 mM MOPS, pH 7.2, 5 mM EDTA, 0.01% lauryl maltoside) using a step-gradient of KCl (0 mM to 250 mM). The fractions containing fumarate reductase were pooled and concentrated (Sartorius Vivaspin 20 50k MWCO followed by Amicon Ultra-0.5 mL Centrifugal Filter).

5.4.4 Expression and purification of *E. coli* cytochrome bo_3

The strain used for expression of His-tagged cytochrome bo3 was used with permission of prof. Robert B. Gennis (University of Illinois) and provided by prof. dr. S. de Vries (Delft University of Technology). The expression and purification of His-tagged cytochrome bo_3 by *E. coli* strain GO105/pJRhisA was based on a literature protocol [20]. A preculture (50 mL LB medium, 100 µg/ml ampicillin) was inoculated with a -80°C stock of *E. coli* GO105/pJRhisA and grown aerobically overnight at 37°C. This culture was

then used to inoculate (10 mL) 2×500 mL of LB medium, supplemented with 50 µg/ml ampicillin and 500 µM $CuSO_4$. Cells were allowed to grow aerobically at 37°C (while shaking) until the mid-logarithmic phase was reached. The cells were then harvested (4°C, 5000 rpm, 20 min, Sorvall RC 6+ centrifuge F105-6x500Y), resuspended (50 mM potassium phosphate, pH 7.5) and again centrifuged (4°C, 5000 rpm, 20 min). The cells were then disrupted using a French press (Stansted 'pressure cell' Homogenizer). The resulting suspension was centrifuged (4000 rpm, 20 min, 4°C, Heraeus Multifuge 3L-R) to remove cell debris. The supernatant was then ultracentrifuged (25000 rpm, 2 hours, 4 °C, Kontron Instruments Centrikon T-1170). The membrane pellets were collected and resuspended in buffer (1-2 mL of 50 mM potassium phosphate, pH 7.5), containing 1% lauryl maltoside, to achieve membrane extraction. After centrifugation (1-2 hrs, max. speed, 4°C, Eppendorf Centrifuge 5415D) the supernatant was diluted with 'buffer A' (50 mM potassium phosphate, 0.05% lauryl maltoside, pH 8.3) and loaded onto a Ni-Sepharose column (5 mL HisTrap FF, GE Healthcare Life Sciences, equilibrated with 'buffer A'). After running the column (4 mL/min, 'buffer A') for several fractions, a step gradient (150 mM imidazole in 'buffer A') was used to elute the enzyme. Fractions were pooled based on color (reddish) and subjected to several rounds of concentration (Sartorius Vivaspin 20 50k MWCO followed by Amicon Ultra-0.5 mL Centrifugal Filter) and subsequent dilution in 'buffer A', until the imidazole concentration was significantly decreased (< 0.2 mM). The concentrated product was divided into portions, flash frozen using liquid nitrogen and stored at -80°C until use.

5.4.5 Expression of DMSO reductase

E. coli DH5α was streaked on an LB agar plate, which was then allowed to grow overnight at 37°C. A colony was picked and used to inoculated 50 mL of LB medium. After 6 hrs of growth at 37°C, 1 mL of this culture was used to inoculate 1 L of minimal glycerol/DMSO medium [36, 37]: 100 mM potassium phosphate buffer pH 6.8; 0.5% glycerol; 15 mM $(NH_4)_2SO_4$; 0.15% casamino acids; 0.003% thiamine-HCl; 5 mM $CaCl_2$; 70 mM DMSO; 60 µM $(NH_4)_6Mo_7O_{24}$; 200 µM $MgSO_4$; 25 mM $MnCl_2$; 1 mM $Fe_2(SO_4)_3$; 0.006%

proline; 0.006% leucine. After 40 hrs of anaerobic growth, the cells were harvested, disrupted and membranes were isolated in an identical fashion as described for cytochrome bo_3.

5.4.6 Estimation of the catalytic rate constant k_{enz}

The following equation (5.1) was used to estimate k_{enz}:

$$k_{enz} = \frac{4N_A R_G^2}{F\Gamma\rho A} i_{cat} \tag{5.1}$$

Here, N_A is Avogadro's number, Γ the electrode surface coverage with enzyme, R_G the radius of gyration of the enzyme, F the Faraday constant, ρ the electrode surface roughness, A the electrode surface area and i_{cat} the catalytic current. Note that Γ and ρ contain considerable uncertainty, i.e. the surface coverage and electrode surface topology are essentially unknown. Nevertheless, full coverage (Γ = 1) and a completely smooth electrode surface (ρ = 1) were assumed. The square of the radius of gyration – an estimation of the electrode surface area occupied by a single enzyme – is defined by equation 5.2.

$$R_G^2 = \frac{1}{2N^2} \sum_{i,j} \left(\vec{r_i} - \vec{r_j}\right)^2 \tag{5.2}$$

Here, N is the number of atoms and r_i is the coordinate vector of an individual atom. Using the protein database file 1NEN [38], containing the crystal structure of succinate dehydrogenase, R_G = 33.69 Å (based on 8297 atoms) was found, which was used to calculate the value k_{enz} = 2.92 s^{-1}.

As can be deduced from this section, prof. dr. Simon de Vries has greatly contributed to the work presented in this chapter. His sudden death both shocked and greatly saddened us. We are very grateful for the fruitful and inspiring collaborations we have had with him.

5.5 References

[1] G Unden, PA Steinmetz, P Degreif-Dünnwald, *EcoSal Plus* **2014**, doi: 10.1128/ecosalplus.ESP-0005-2013

[2] LL Yap, MT Lin, H Ouyang, RI Samoilova, SA Dikanov, RB Gennis, *Biochimica et Biophysica Acta* **2010**, 1797, 1924–1932

[3] H Wang, CP Tseng, RP Gunsalus, *Journal of bacteriology* **1999**, 181, 5303-5308

[4] OS Ksenzhek, SA Petrova, MV Kolodyazhny, *Bioelectrochemistry and Bioenergetics* **1982**, 9, 167-174

[5] K Takehara, Y Ide, *Journal of Electroanalytical Chemistry and Interfacial Electrochemistry* **1991**, 321, 297-305

[6] K Kita, CRT Vibat, S Meinhardt, JR Guest, RB Gennis, *Journal of Biological Chemistry* **1989**, 264, 2672-2677

[7] JA Cracknell, KA Vincent, FA Armstrong, *Chem. Rev.* **2008**, 108, 2439–2461

[8] VWT Cheng, "Electron Transfer and Quinone Chemistry in *Escherichia coli* Dimethyl Sulfoxide Reductase and Succinate Dehydrogenase", *PhD Thesis*, *University of Alberta*, **2008**

[9] G Cecchini, I Schröder, RP Gunsalus, E Maklashina, *Biochimica et Biophysica Acta* **2002**, 1553, 140–157

[10] E Maklashina, G Cecchini, *Biochimica et Biophysica Acta* **2010**, 1797, 1877–1882

[11] VWT Cheng, RS Piragasam, RA Rothery, E Maklashina, G Cecchini, JH Weiner, *Biochemistry* **2015**, 54, 1043–1052

[12] BAC Ackrell, *FEBS letters* **2000**, 466, 1-5

[13] CG Mowat, R Moysey, CS Miles, D Leys, MK Doherty, P Taylor, MD Walkinshaw, GA Reid, SK Chapman, *Biochemistry* **2001**, 40, 12292–12298

[14] JM Hudson, K Heffron, V Kotlyar, Y Sher, E Maklashina, G Cecchini, FA Armstrong, *J. Am. Chem. Soc.* **2005**, 127, 6977–6989

[15] CC Moser, TA Farid, SE Chobot, PL Dutton, *Biochimica et Biophysica Acta* **2006**, 1757, 1096–1109

[16] CC Page, CC Moser, PL Dutton, *Current Opinion in Chemical Biology* **2003**, 7, 551-556

[17] J Ma, A Katsonouri, RB Gennis, *Biochemistry* **1997**, 36, 11298–11303

[18] J Abramson, S Riistama, G Larsson, A Jasaitis, M Svensson-Ek, L Laakkonen, A Puustinen, S Iwata, M Wikström, *Nature Structural Biology* **2000**, 7, 910-917

[19] A Puustinen, MI Verkhovsky, JE Morgan, NP Belevich, M Wikstrom,

Proc. Natl. Acad. Sci. USA **1996**, 93, 1545-1548
[20] JN Rumbley, EF Nickels, RB Gennis, *Biochimica et Biophysica Acta* **1997**, 1340, 131-142
[21] N Ray, J Oates, RJ Turner, C Robinson, *FEBS letters* **2003**, 534, 156-160
[22] P Geijer, JH Weiner, *Biochimica et Biophysica Acta* **2004**, 1660, 66-74
[23] K Heffron, C Léger, RA Rothery, JH Weiner, FA Armstrong, *Biochemistry* **2001**, 40, 3117-3126
[24] C Iobbi-Nivol, S Leimkühler, *Biochimica et Biophysica Acta* **2013**, 1827, 1086-1101
[25] FA Armstrong, *J. Chem. Soc.*, *Dalton Trans.* **2002**, 661-671
[26] M Kasahara, Y Anraku, *Journal of biochemistry* **1974**, 76, 959-966
[27] BA Ackrell, B Cochran, G Cecchini, *Arch. Biochem. Biophys.* **1989**, 268, 26-34
[28] E Lohmeier, DS Hagen, P Dickie, JH Weiner, *Canadian Journal of Biochemistry* **1981**, 59, 158-164
[29] E Maklashina, RA Rothery, JH Weiner, G Cecchini, *Journal of Biological Chemistry* **2001**, 276, 18968-18976
[30] VW Cheng, RA Rothery, MG Bertero, NC Strynadka, JH Weiner, *Biochemistry* **2005**, 44, 8068-77
[31] E Maklashina, G Cecchini, *Arch. Biochem. Biophys.* **1999**, 369, 223-232
[32] SA Weiss, RJ Bushby, SD Evans, LJC Jeuken, *Biochimica et Biophysica* **2010**, 1797, 1917-1923
[33] WR Hagen, *Eur. J. Biochem.* **1989**, 182, 523-530
[34] SGH Rossius, "Internal electron transfer rates in *E. coli* fumarate reductase", *MSc Thesis*, *Delft University of Technology*, **2011**
[35] ME Spencer, JR Guest, *Journal of Bacteriology* **1974**, 117, 947-953
[36] D Sambasivarao, JH Weiner, *Journal of Bacteriology* **1991**, 173, 5935-5943
[37] PT Bilous, JH Weiner, *Journal of Bacteriology* **1985**, 162, 1151-1155
[38] V Yankovskaya, R Horsefield, S Tornroth, C Luna-Chavez, H Miyoshi, C Leger, B Byrne, G Cecchini, S Iwata, *Science* **2003**, 299, 700-704, doi: 10.2210/pdb1nen/pdb